

B. Broder^{1,2}, M.S.Freeman²

¹Department of Radiology and Committee on Medical Physics, The University of Chicago, Chicago, Illinois 60637, USA

²Los Alamos National Laboratory, Los Alamos, New Mexico 87545, USA

ABSTRACT

Proton radiography could provide a real-time imaging modality for proton therapy, allowing patients to be more accurately positioned and more thoroughly exploiting the specific dose-deposition properties of protons as characterized by a Bragg peak. In this project, a system is modeled after the 800-MeV proton radiography (pRad) system at the Los Alamos Neutron Science Center (LANSCE), using the TOOl for PArticle Simulation (TOPAS).^[4] All imaging system components of the LANSCE pRad system were modeled, as well as several phantoms typically used in quality assurance testing of medical imaging modalities. Several contrast agents were placed in these phantoms to determine the optimal agent for an experimental study. Modeling of water, Gallium-68, and gold showed that the latter two agents would be suitable for proton imaging, while water would not provide enough contrast.

Since TOPAS employs a hierarchy of text files, a user could easily place their own phantom into the pRad system and determine the viability of their own experiment. By incorporating the physics of Geant4 in a user friendly package for Monte Carlo simulations of proton and heavy ion therapy treatments, a TOPAS model could become easy to deploy as open source tools to be utilized by the medical community.

INTRODUCTION

Proton radiography, based off of a magnetic lens system [1, 2], can provide instantaneous estimations of proton stopping power that could be used to make real-time adjustments to a patient's treatment plan to accommodate changes in anatomy that can occur on a daily basis.^[3] Such a system exploits the charge of the proton to focus an image to a focal point downstream of the patient; collimation at a Fourier plane within the lens provides a high level of sensitivity to changes in patient thickness.

The resolution of such a system is sensitive to 1. the spread in energies of transmitted protons vs. the focal energy of the lens and 2. the amount of multiple-Coulomb scattering acquired as the proton traverses a patient. For these reasons, instantaneous proton radiography is better suited to operate at higher energies to minimize both scatter and dE/E. At present, a patient's dose map is calculated with X-ray imaging. Inferring proton stopping energy from X-rays comes at the expense of an error of $\pm 2\%$. By providing a value of proton stopping power based on the water equivalent path length and transmission of the image, proton radiography gives a specific value of proton stopping power for an image, drastically improving upon the above error threshold.

Here, a system is modeled after the 800-MeV proton radiography system at the Los Alamos Neutron Science Center (LANSCE), using the TOOl for PArticle Simulation (TOPAS).^[4] TOPAS incorporates the physics of Geant4 in a user friendly package for Monte Carlo simulations of proton and heavy ion therapy treatments. Models developed in TOPAS are thus relatively easy to deploy as open source tools to be utilized by the medical community.



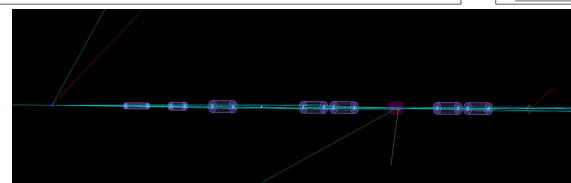
Figure 1: The proton beam trajectory for the LANSCE pRad system. After the object, the beam becomes scattered. The lenses sort the beam scattering by angle. At the collimator, the greatest scattered portions of the beam are removed. The remaining beam is then focused on the detector.

MATERIALS AND METHODS

Proton Radiography System

The lens-based proton radiography (pRad) system was designed using the differential algebraic-based beamline design code, COSY INFINITY.^[5] To replicate the proton flux of the system at LANSCE in TOPAS, 10^7 particles were used per simulation. The beam spread is a Gaussian with $\sigma = 0.85$ cm. The pRad system begins with a tantalum diffuser foil. The beam is then formed in three quads to provide the matching conditions to produce a Fourier plane within the downstream lens system. A phantom is imaged through a lens constructed of four magnetic quadrupoles, which were vacuum cylinders with electromagnetic field gradients. The 15 cm \times 15 cm \times 0.2 cm detector is divided into 1500 \times 1500 \times 1 bins and consists of LYSO. The amount of energy deposited in each bin was scored.

An intensity image of energy per bin was generated in Python. Image flattening was done by dividing the phantom image by an image of the beam with no phantom present. Adjustments were made to each image in ImageJ to optimize visibility.



Phantoms

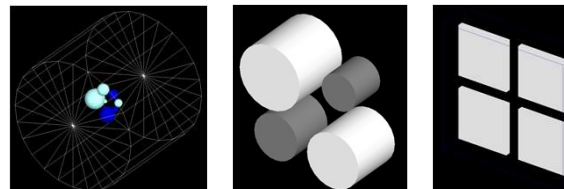
At the imaging plane, several phantoms were used to assess the resolution of the system and amount of contrast agent needed to produce an image. Phantoms were designed to be similar to those used in quality assurance testing for traditional imaging modalities such as SPECT (Single Photon Emission Computed Tomography) and PET (Positron Emission Tomography).

Table I: Phantom Descriptions

Phantom	Description	Dimensions	Material	Density
Jaszczak sphere phantom	Water spheres in a vacuum cylinder	Diameters: 9.5, 12.7, 15.9, 19.1, 25.4, 31.8 mm	Water, Gold, or Gallium	Water: 1.000 g/cm ³ Gold: 19.32 g/cm ³ Ga68: 5.91 g/cm ³
Cylinder Phantom	Water cylinders	Diameters: 2, 2.5, 3, 3.5 cm; length: 3.5 cm	Water	1.000 g/cm ³
Box Phantom	Lead boxes in a vacuum box	Box length: 2 cm x, 2 cm y, 0.2 cm z	Lead	11.35 g/cm ³

Figure 2: A bird's-eye view of the pRad system with a low number of counts. On the far left is the tantalum diffuser, followed by three beam-forming quadrupoles. After the object plane, two sets of two quadrupoles are separated by a collimator (dark purple) before reaching the detector at the far right. The teal lines are proton trajectories, while the other lines are scattered particles such as electrons, neutrons, or photons.

Figure 3: Imaging phantoms used in the proton radiography system. In medical imaging, they are used to assess things such as resolution and contrast. From left to right: Jaszczak phantom, cylinder phantom, and box phantom. Specifications are provided in Table 1.



RESULTS

Effect of Collimator

The purpose of a collimator is to reduce the multiple Coulomb scattering, thereby creating a clearer image. The collimator effect is shown in the middle column (increasing collimation from top to bottom). With increasing collimation, the images are darker and more well-defined. The effect is most pronounced between no collimation and other collimators.

Effect of Phantom

Different phantoms are composed of different materials and dimensions, thereby providing different levels of contrast. Phantom effect is shown in the middle row. The lead phantom is the most visible, and the water cylinder phantom is the least visible. The cylinder phantom is more visible than the Jaszczak water phantom due to the cylinder depths compared to sphere diameters.

Effect of Contrast Agent

Since proton radiography is a transmission imaging modality, strong differences in proton absorbance provide greater contrast. The three contrasts primarily studied (68Ga, Au, and water) have much different numbers of protons (Z) and masses. Contrast effect is shown on the bottom row (left to right increasing Z).

Figure 5: 1, 3, and 6 show no, 5 and 10 mrad, respectively, collimator effects of a 68Ga Jaszczak phantom. 2-4 show a water cylinder, 68Ga Jaszczak, and lead box phantom, all with a 5 mrad collimator. Both the phantom

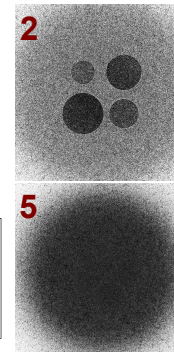


Figure 5. (cont): Material (Z) and depth contribute to their visibility. 5-7 show the effect of water (5), 68Ga (6) and gold (7) contrast in a 10 mrad Jaszczak phantom. Both 68Ga and Au are visible, but Au has better contrast.

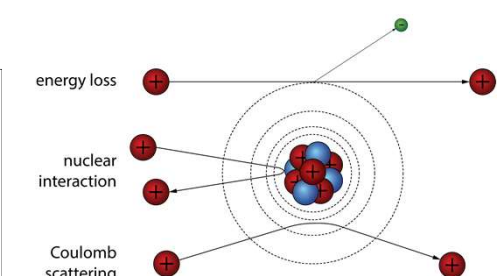
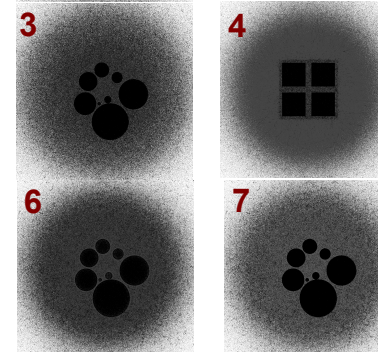


Figure 4: Possible proton interactions. Coulomb scattering (bottom) is shown by the multi-colored lines in Figure 1 and causes scattering at different angles corresponding to different energies. The nuclear reactions (middle) create different particles upon interaction, such as the neutrons or electrons seen in Figure 2. Energy loss (top) is used for transmission radiography: as a proton deposits dose and loses energy, it slows down.

DISCUSSION AND FUTURE WORK

TOPAS provided an effective platform to design Geant4-based Monte Carlo simulations of proton radiography. Based on the images in the bottom row of Figure 4, gold was determined to have the highest level of contrast. However, 68Ga still had an acceptable level of contrast such that it could be distinguishable for proton imaging. Results confirmed the poor tissue contrast seen in proton radiography using water as a tissue-equivalent material. The collimator was also shown to have a significant effect, with the most notable difference being between no collimator and any collimator.

Future work will focus on validating these results experimentally using a mouse model with 68Ga-DOTATE and gold nanoparticles serving as contrast agents. Results of these studies can be confirmed using CT (computed tomography), MRI (magnetic resonance imaging), and PET due to the dual-modality nature of these tracers. In simulations, more accurate phantoms will be created by placing the contrast spheres in a water phantom, as is done with a real Jaszczak phantom. Additionally, the level of material needed to provide a visible signal will be assessed to determine the minimum amount of contrast agent needed for experimental studies.

ACKNOWLEDGEMENTS

This work was supported by Los Alamos National Laboratory LDRD under DOE/NNSA contract DE-AC52-06NA25396. This project was also supported in part by the National Physical Sciences Consortium as part of the NPSF Fellowship.

REFERENCES

- [1] N. King, E. Ables, et al., "An 800-MeV proton radiography facility for dynamic experiments," *Nucl. Instrum. Meth. A* 424, 84-91 (1999).
- [2] C.T. Mottershead, J.D. Zumbro, presented at the Part. Accel. Conf., Vancouver, BC, 1997 (unpublished).
- [3] D. Yan, F. Vicini, et al., "Adaptive radiation therapy," *Physics in Medicine & Biology* 42, 123 (1997).
- [4] J. Perl, J. Shin, et al., "TOPAS: an innovative proton Monte Carlo platform for research and clinical applications," *Medical physics* 39, 6818-6837 (2012).
- [5] K. Makino, M. Berz, "Cosy infinity version 9," *Nucl. Instrum. Meth. A* 558, 346-350 (2006).